Proceedings of the ASME 2024
15th International Pipeline Conference
IPC2024
September 23-27, 2024, Calgary, Alberta, Canada

IPC2024-134184

ADVANCING LEAK DETECTION IN NATURAL GAS PIPELINES: A NOVEL APPROACH USING REAL-TIME TRANSIENT MODELING FOR METHANE EMISSIONS MITIGATION

Hamed Ghasvari-Jahromi[1,†,*], Fatemeh Ekram[1,†], Satya Mokamati[1]

[1]Vanmok Leak Detection Technologies Inc., Edmonton, Alberta, Canada

ABSTRACT

Currently, methane emissions account for approximately 25% of human-induced global warming, with the oil and gas sector ranking among the leading contributors. Early detection of methane leaks in pipelines significantly reduces the greenhouse gases emissions, aiding in the mitigation of adverse economic and environmental consequences associated with climate change. Computational Pipeline Monitoring (CPM) systems, tailored for leak detection, provide continuous pipeline monitoring and offer early identification of leaks while minimizing false alarms. This study harnesses advancements in tracking and estimation methodologies and integrates them with physics-based models to address the intricacies of modeling gas pipelines and introduces a real-time transient model (RTTM) used for leak detection of natural gas pipelines.

Keywords: Real time transient modeling, Pipeline leak detection, Bayesian filtering, Natural gas transportation, Methane emissions reduction

NOMENCLATURE

ρ	Density [kg m^{-3}]
v	Velocity [m s^{-1}]
D	Pipe diameter [m]
P	Pressure [Pa]
f	friction factor
g	Gravitational acceleration [m s^{-2}]
u	Specific internal energy[J kg^{-1}]
h	Specific enthalpy[J kg^{-1}]
T	Temperature [K]
q	Specific heat flow rate [J kg^{-1} s^{-1}]
x	Distance along the pipe [m]
t	Time [s]
α	Pipe inclination angle
R	Universal gas constant [J mol^{-1} K^{-1}]
k	Thermal conductivity [W m^{-1} K^{-1}]
α	Thermal diffusivity [m^2 s^{-1}]
μ	dynamic viscosity [Pa.s]
ν	Kinematic viscosity [m^2 s^{-1}]
c_p	specific heat at constant pressure [[J kg^{-1} K^{-1}]
c_v	specific heat at constant volume [[J kg^{-1} K^{-1}]

1. INTRODUCTION

Addressing methane emissions emerges as an important part of global efforts to mitigate climate change. Over a span of a century, methane is estimated to have a global warming potential (GWP) around 28-36 times greater than that of carbon dioxide. This means that, molecule for molecule, methane heat-trapping effect far exceeds carbon dioxide.

The regulations and policies are in place to reduce methane emissions from the oil and gas sector to mitigate the negative economic and environmental impacts of climate change. Methane emissions from pipeline refers to the unintentional release of methane, the principal component of natural gas. Such leaks can occur for various reasons, including equipment failure, corrosion, construction defects, or inadequate maintenance.

A study, published in the Proceedings of the National Academy of Sciences, monitored methane emissions in the Boston area for 8 years, starting from 2012 to 2020. It is found that an average of 49,000 tons of methane leaked into the air each year. That accounts to an estimated 2.5% of all gas delivered to the metro area and is equivalent to the carbon dioxide emissions from roughly a quarter-million cars operating for a year.

The emissions from ruptures in high-pressure gas pipelines are substantial. According to The United Nations Environment Program (UNEP), it is estimated that between 75000 to 230,000 tons of methane leaked during the incident on the Nord Stream natural gas pipelines in September 2022. This is equivalent to 2.1 to 6.44 million tons of CO_2. An effective leak detection algorithm can minimize the adverse impacts of the methane leakage if an incident occurs.

Pipelines carrying methane are present at different stages of oil and gas industry. The gathering pipelines collect petroleum

[†]Joint first authors
*Corresponding author: hamed@vanmok.com

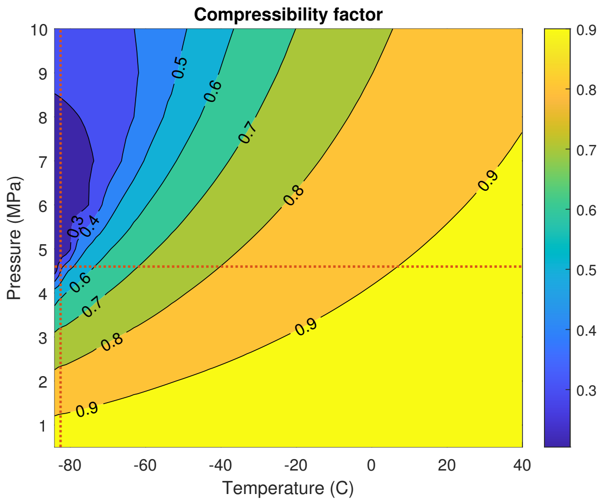

FIGURE 1: COMPRESSIBILITY FACTOR FOR DIFFERENT TEMPERATURE AND PRESSURES

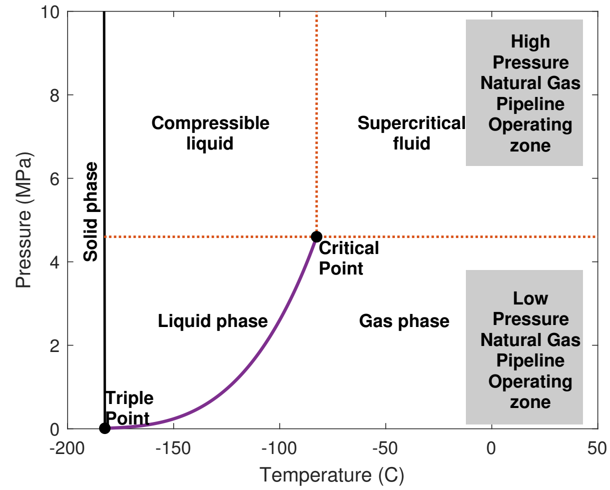

FIGURE 2: METHANE PHASE DIAGRAM

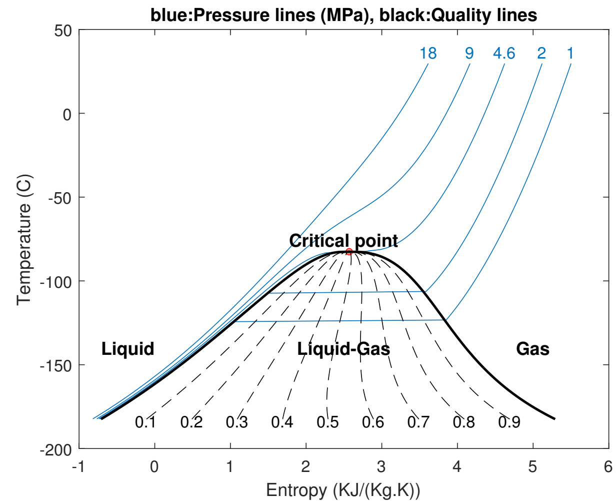

FIGURE 3: METHANE TEMPERATURE- ENTROPY (TS) DIAGRAM

emulsions and raw natural gas from extraction wells within a production field and transport it to processing facilities. Gathering pipelines typically have small-medium diameter and operate at low-medium pressures.

Transmission pipelines transport processed natural gas over long distances, often across state or national borders and even extending offshore. These pipelines operate at higher pressures to facilitate the efficient movement of high volumes of products over vast distances.

Distribution pipelines deliver natural gas from transmission lines to end-users, such as residential, commercial, and industrial customers. Distribution pipelines operate at relatively low pressures and are typically found in urban and suburban areas.

Efforts to minimize methane pipeline leakage are crucial not only for environmental reasons but also for ensuring the safety and integrity of the natural gas infrastructure. Regulatory authorities and industry stakeholders work together to establish and enforce standards aimed at preventing and addressing pipeline leaks.

Computational Pipeline Monitoring (CPM)-based leak detection systems using real-time transient model (RTTM) of the pipeline, widely adopted for liquid pipelines [1–3]. Despite challenges in applying CPM to gas pipelines due to inherent complexities, recent developments offer promising solutions. Significant advances in data collection, data-driven methodologies and technology over the past few years have greatly increased our ability to detect and quantify methane releases due to leaks in pipelines.

Availability of reliable and cost-effective CPM-based leak detection systems are imperative as they offer several benefits including continuous pipeline monitoring and early identification of leaks while minimizing false alarms. This paper provides insights into the state-of-the-art approaches for methane leak detection in natural gas pipelines using real-time transient modeling of the pipeline.

The following section offers an insight into the modeling approach adopted to simulate the dynamics of natural gas pipelines, underscoring the imperative of integrating an equation of state for real-time computation of fluid density in natural gas systems.

Section 3 describes the integration of the state estimators into the model to advance the predictions amidst uncertainties and limited measurements. Section 4 delves into the feasibility and constraints associated with deploying a real-time transient model (RTTM)-based leak detection system employing particle filters.

The results and discussion section presents the findings of the case studies for the purpose of model validation and illustrating the improvements facilitated by the application of particle filters. Finally, the paper is concluded.

2. MODELING OF NATURAL GAS PIPELINES

The pipeline model solves a system of partial differential equations (PDEs) include the conservation laws of mass, momentum and energy [4].

Starting with the three conservation laws— continuity, momentum, and energy—, the numerical solution for hyperbolic partial differential equations (PDEs) can be achieved as described

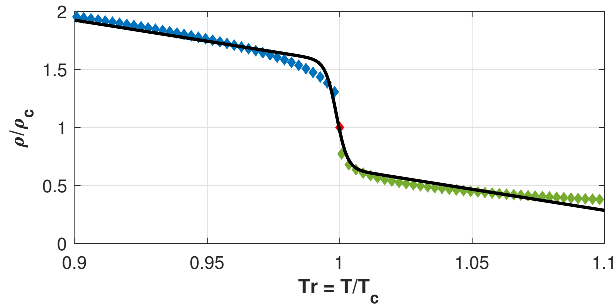

FIGURE 4: REDUCED DENSITY VS T_r AT P_{cr} (DOTS) AND THE FITTED CURVE (SOLID LINE).

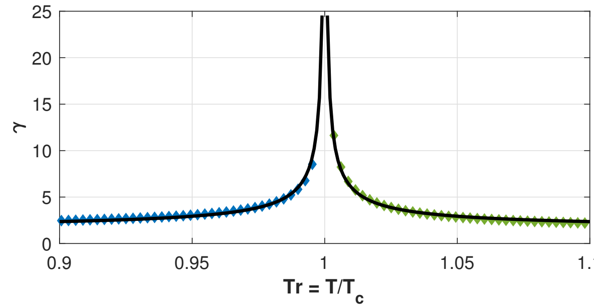

FIGURE 6: HEAT CAPACITY RATIO VS T_r AT P_{cr} (DOTS) AND THE FITTED CURVE (SOLID LINE).

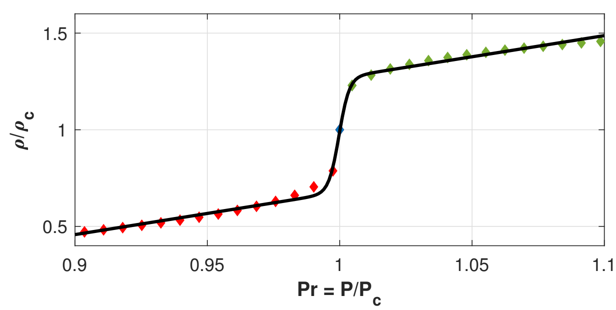

FIGURE 5: REDUCED DENSITY VS P_r AT T_{cr} (DOTS) AND THE FITTED CURVE (SOLID LINE).

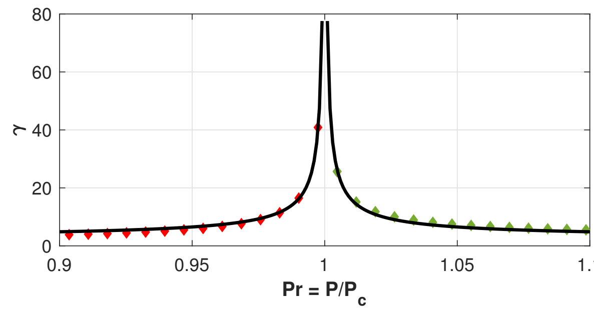

FIGURE 7: HEAT CAPACITY RATIO VS P_r AT T_{cr} (DOTS) AND THE FITTED CURVE (SOLID LINE).

in [5, 6].

$$\frac{\partial \rho}{\partial t} + \frac{\partial(\rho v)}{\partial x} = 0 \tag{1}$$

$$\frac{\partial(\rho v)}{\partial t} + \frac{\partial(P + \rho v^2)}{\partial x} = -\frac{f\rho v|v|}{2D} - \rho g sin\alpha \tag{2}$$

$$\frac{\partial}{\partial t}\left[\left(u + \frac{v^2}{2}\right)\rho\right] + \frac{\partial}{\partial x}\left[\left(h + \frac{v^2}{2}\right)\rho v\right] = \rho q - \rho v g sin\alpha \tag{3}$$

2.1 Equation of State

To effectively detect leaks in pipelines with compressible flow, it's essential to calculate density in real-time. This requires integrating an auxiliary equation of state into the model to establish density as a function of pressure and temperature. For natural gas, the density can be described by $P = Z\rho RT$, in which Z is the compressibility factor and can be obtained from available equation of states (EOS).

Figure 1 illustrates the compressibility factor of methane derived from the Setzmann and Wagner equation of state [7]. It's evident from the graph that deviations from the ideal gas law are most when pressures and temperatures surpass the critical point and real gas effects must be considered. This is the case for transmission pipelines where the line operates above the critical point of -82.6°C and 4.6 MPa.

As we discussed in [5] and [6], to achieve the best accuracy and minimize the computational effort from an equation of state, the best approach especially for the dense phase fluid in the pipeline is the correctional correlations, which are derived from thermal properties of matter and shaped into thermodynamics functional. This functional becomes an auxiliary equation like a constitutive equation. The same approach is applied for this study.

2.2 Thermodynamic phases

In the natural gas pipeline, thermodynamic phases refer to the different states of matter that the gas can exist in under varying operating pressures and temperatures. Figure 2 shows the phase diagram for methane as the main component of natural gas. The critical point of methane is at -82.6°C and 4.6 MPa. If the pipeline operates below the critical pressure, and assuming that the operating temperature of the pipeline is above the critical temperature, then methane is in its gaseous phase. This scenario is typical for gathering and distribution pipelines.

In contrast, the transmission pipelines operate at elevated pressures, transporting methane in its supercritical state. Supercritical fluids exhibit densities akin to liquids and viscosities similar to gases. Modeling gas flow in the supercritical region demands additional considerations, as detailed subsequently.

Figure 3 is a T-S diagram, illustrating the changes in temperature and entropy of methane. The saturation curve, depicted as the black line, represents the boundary between the liquid phase and the vapor phase at equilibrium. It delineates the conditions under which the substance can exist simultaneously as both a liquid and a vapor. Isobaric lines, denoting different pressures, are also depicted in blue. The dashed black lines are quality lines representing the gas farction of the liquid-gas phase.

TABLE 1: PARAMETERS FOR THE REDUCED DENSITY CORRELATION

x	y	R^2	a	b	c	d	k
T_r	ρ_r	0.99	4.28	-3.64	0.91	1.84	-493.3
P_r	ρ_r	1.00	-1.51	2.19	0.59	0.88	519.8

TABLE 2: PARAMETERS FOR THE HEAT CAPACITY RATIO CORRELATION

x	y	R^2	γ_{max}	a	b	c
T_r	γ	0.99	24.54	0.09	1.43	0.7
P_r	γ	0.99	77.55	0.34	2.37	0.74

2.3 Supercritical Region

A discontinuity in tabulated thermodynamic properties occurs as the fluid passes through the critical point. In this study, regularization techniques are employed to establish correlations that allow for the continuous determination of fluid properties throughout the transition across the critical point and into the supercritical region. These correlations enable the calculation of properties at critical pressure as a function of reduced temperature (T_r) and at critical temperature as a function of reduced pressure (P_r).

These relationships encompass various substances beyond methane, including ethane, propane, butane, and CO2 [5]. Augmented with conservation equations of mass, momentum, and energy, these correlations form a comprehensive model for dense phase transportation in pipelines.

Equations 4 and 5 denote the correlations for the reduced density and heat capacity ratio of methane, respectively. The parameters for these equations are provided in Table 1 and 2.

$$\rho_r = a + bx + \frac{c}{1 + de^{-k(x-1)}} \tag{4}$$

$$\gamma = b + |\frac{a}{x-1}|^c \tag{5}$$

Figures 4 and 5 depict the reduced density as a function of T_r and P_r, respectively. The heat capacity correlation for T_r and P_r as independent variables are presented in figures 6 and 7.

2.4 Model Verification

Initial verification of the model is performed using existing experimental data from the literature. The isothermal conditions with a constant temperature along the pipe is assumed for the following cases. After discussing the possible advancement in the model in the following sections, the final validation of the advanced model's performance, using data from an industrial pipeline will be presented in the results and discussions section.

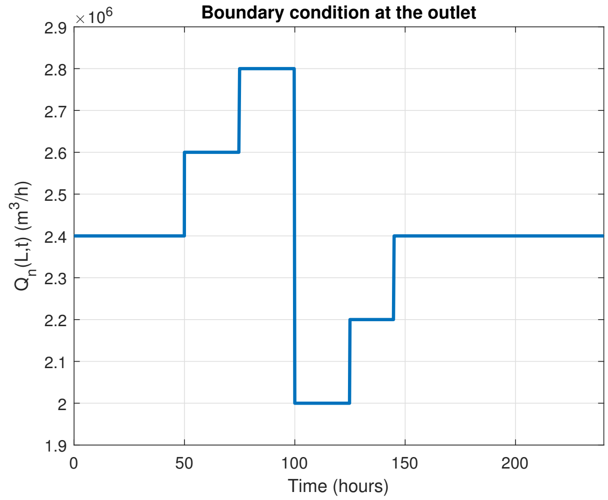

FIGURE 8: BOUNDARY CONDITION FOR THE OUTLET FLOW RATE

2.4.1 Case Study 1. The proposed model was used to simulate a pipeline under identical setup and boundary conditions as those employed by Chaczykowski [8]. While Chaczykowski's boundary conditions were arbitrarily chosen, they accurately reflect common flow conditions observed in natural gas transmission pipelines.

The pipeline is 363 km long with diameter of 1383.6 mm and wall thickness of 19.22 mm. The pipe roughness is considered to be 0.0015 mm.

The molar composition of the gas is CH_4 (98.3455%), C_2H_6 (0.6104%), C_3H_8 (0.1572%), $i - C_4H_{10}$ (0.0299%), $n - C_4H_{10}$ (0.0253%), $i - C_5H_{12}$ (0.0055%),$n - C_5H_{12}$ (0.0040%), N_2 (0.0303%) and CO_2 (0.7918%). The density of the mixture is $\rho_n = 0.7347\ kg/m^3$ at normal temperature and pressure.

The pipeline is buried at the depth of 1.5 m and the ground temperature is 3.1 °C. Soil thermal conductivity and density are $k = 1.0W/m.K$ and $\rho = 1640kg/m^3$ respectively. The pipe material is steel with the following properties: $k = 45.3W/m.K$, $\rho = 7830kg/m^3$ and $c_p = 500J/kg.K$. The pipe has an internal and external coating with know properties reported in [8].

The pipeline inlet pressure and temperature are assumed to be at 8.4 MPa and 296.65 K. The boundary condition for the outlet flow rate at normal pressure and temperature is presented in figure 8, as was applied in [8]. The pressure at the outlet and the flow rate at the inlet were calculated using the proposed model in this study and compared with the results from [8].

Figure 9 shows the normal flow rate at the inlet . Figure 10 shows the pressure at the outlet. The blue lines are the calculation from our model compared to the results from [8] depicted by black dots.

2.4.2 Case Study 2. The operating pressure for the first case study was above the critical pressure of methane and the fluid was transported in its supercritical state. In this case study we selected a pipeline with operating pressure below the critical point which means that methane is in gaseous phase. The pipeline has the length of 80 miles and diameter of 18 inches carrying 1500 MSCFH of natural gas. This pipeline was used by the London

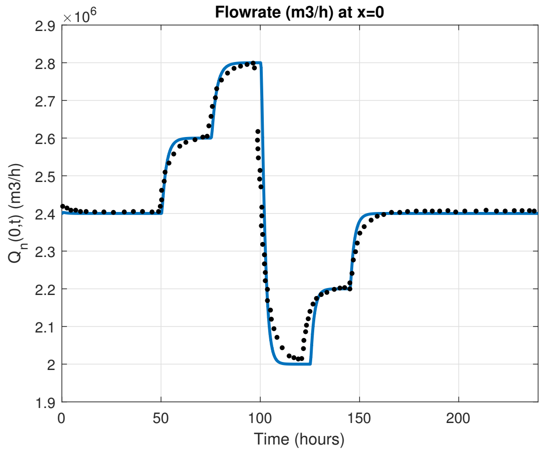

FIGURE 9: COMPARISON OF THE CALCULATED INLET FLOW RATE (SOLID BLUE LINE) WITH CHACZYKOWSKI [8] (BLACK DOTS)

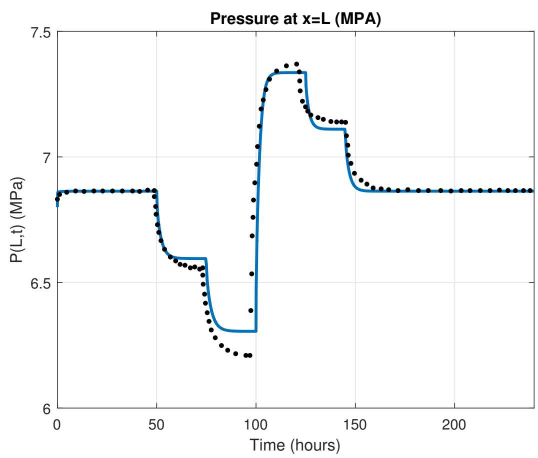

FIGURE 10: COMPARISON OF THE CALCULATED OUTLET PRESSURE (SOLID BLUE LINE) WITH CHACZYKOWSKI [8] (BLACK DOTS)

research service (LRS) for demonstration and was discussed in [9]. The pipeline is in a steady state at the beginning of the simulation before the flow rate was increased by 50% and stayed the same for the rest of the simulation time. The inlet pressure kept constant at 350 psig (2.5 MPa). The calculated outlet pressure is drawn in figure 11. The pressure dropped to a new steady state value as the result of the increased flow rate, which is in agreement with the results from [9].

3. ADVANCING MODEL PREDICTIONS THROUGH STATE ESTIMATORS

Models often developed based on some assumptions and their ability to accurately capture different aspects of the system dynamics depends on validity of those assumptions. The uncertainties in the model parameters and inherent noise in the measurements, affect the model predictions even for the most comprehensive models.

In this section we investigate the integration of advanced

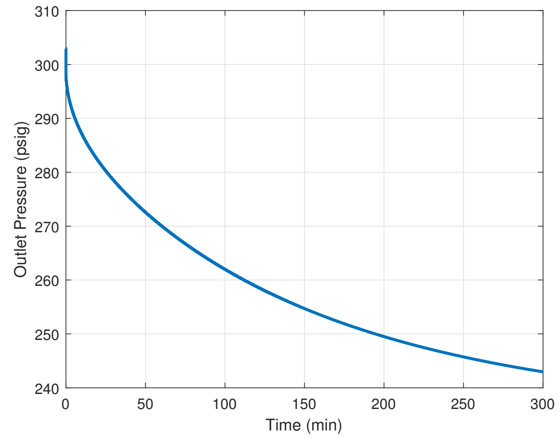

FIGURE 11: THE CALCULATED OUTLET PRESSURE FOR CASE STUDY 2.

state estimation techniques into the model to improve its predicting ability despite the complexities and uncertainties due to unknowns and noises.

To better explain the components of the state estimation algorithm, we use the state space representation of the model. In a state-space model, the dynamics of a system are represented by a set of state equations (f) and observation equations (h). The state-space model can be represented in matrix form as follows:

$$\begin{aligned} x_{t+1} &= f(x_t, u_t, \epsilon_t) \\ z_t &= h(x_t, \delta_t) \end{aligned} \tag{6}$$

Where x_t is the state vector, u_t is the control input vector, ϵ_t is the process noise vector, z_t is the measurement vector, and δ_t is the measurement noise vector.

Figure 12 represents the block diagram of state estimator coupled with the model to enhance the predictions and benefits the leak detection system. The key components typically found in such a diagram are as follows:

- ***State vector** (x_t)* consists of the values of pressure (P), velocity (v), temperature (T), and density (ρ) at each computational node along the pipe at time t.

- ***Input vector** (u_t)* involves the available boundary conditions at the inlet and outlet of the pipeline.

- ***Measurements vector** (z_t)* contains the observed measurements of the pipeline obtained from sensors or other measurement devices. These measurements provide information about the pipeline's behavior but may be subject to noise, errors, or limitations. The measurement vector serves as the primary input to the state estimator and is used to update the estimate of the system's state.

- ***Process noise** (ϵ_t)* originates from inherent randomness or disturbances in the system dynamics that are not accounted for in the model. These disturbances could stem from external factors such as environmental variability, unmodeled interactions, or stochastic processes influencing the system's behavior.

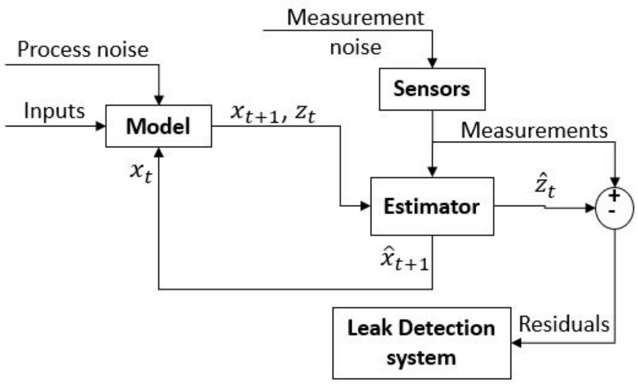

FIGURE 12: STATE ESTIMATOR BLOCK DIAGRAM.

- ***Measurement noise (δ_t)*** is present due to sensor inaccuracies, environmental interferences or communication errors in SCADA systems.

- ***Model*** represents the mathematical description of the pipeline including the conservation laws of mass, momentum and energy along with the equation of state. The model predicts the state vector at the next time-step (x_{t+1}) and the current measurement vector (z_t).

- ***State estimator*** is the core component of the block diagram responsible for estimating the system's state based on available measurements and the system model. It employs estimation algorithms, to recursively update the state estimate over time. The state estimator combines information from the system model and measurements to minimize the discrepancy between predicted and observed states, providing an optimal estimate of the true system state even in presence of uncertainties associated with the model parameters and measurements.

- ***Estimated state ($\hat{x}_{t+1}$)*** is the output of the state estimator, representing the estimated state of the system based on the available measurements and the system model. It provides an approximation of the true system state and is used for monitoring, control, decision-making including leak detection.

- ***Residuals*** are the differences between predicted measurements based on the state estimate ($\hat{z}_t$)), and the actual observed measurements from sensors. Residuals are used for diagnostic purposes, detect abnormalities or faults in the system such as leak.

When it comes to the selection of estimation algorithm for the pipeline model, the ability of the algorithm to address the nonlinearity of the model plays important role in the successful implementation of the estimator.

Particle filters are a type of Bayesian filtering and a powerful state estimation algorithm to deal with variety of the uncertainties. Comparing to the traditional state estimators like the Kalman filter, particle filters, can handle non-linear and non-Gaussian systems, making them applicable in wide range of real-world problems. Particle filters are non-parametric and they don't assume any particular shape for the distribution of the state variables. Instead, they represent the distribution using a collection of discrete samples called particles. This gives us the opportunity to consider the nature of the variable when choosing the probability distribution.

These particles are akin to hypothetical scenarios of the system's state variables. They're generated based on the available information about the system's dynamics and the measurements received from sensors. Each particle represents a possible state variable of the system. The more particles there are, the more finely the state space is represented.

The heart of particle filters lies in Monte Carlo sampling techniques. At each time step, particles are initially generated from a prior distribution, typically based on the known dynamics of the system. These particles are then propagated forward in time according to the system's dynamics model.

When new measurements become available, each particle's likelihood given the measurements is evaluated. This reflects how well each particle agrees with the observed data. Particles that are consistent with the measurements are assigned higher weights, while those that are not are given lower weights.

To prevent the filter from becoming dominated by a few particles, a re-sampling step is performed. In re-sampling, particles with higher weights are more likely to be replicated, while those with lower weights are discarded. This process ensures that particles are distributed more evenly according to their likelihoods.

By combining information from multiple particles, each representing a potential state of the system, particle filters provide an estimate of the system's true state along with an associated uncertainty. This estimate is updated continuously as new measurements arrive, making particle filters suitable for real-time applications where the state of the system needs to be tracked over time despite uncertainties in the system's behavior and the measurements obtained from sensors.

By representing the state-space model in probabilistic form, we can explicitly account for uncertainties and model stochastic processes, which is essential for probabilistic filtering algorithms such as the particle filter. The state-space model in probabilistic form involves specifying both the state and observation equations in terms of their conditional probability distributions:

$$\begin{aligned} p(x_{t+1}|x_t, u_t) &= \mathcal{N}(x_{t+1}; f(x_t, u_t), Q_t) \\ p(z_t|x_t) &= \mathcal{N}(z_t; h(x_t), R_t) \end{aligned} \tag{7}$$

where $\mathcal{N}$ denotes the normal distribution, f is the state function, Q_t is the process noise covariance matrix, h is the measurement function, and R_t is the measurement noise covariance matrix.

The following algorithm outlines the steps involved in state estimation using a particle filter. More details can be found in [10–12].

1. ***Initialization:***

   - *Initialize Particles:* Generate an initial set of particles representing the possible states of the system. Each particle $x_t^{(i)}$ includes the state variables of interest at time t and their associated weights $w_t^{(i)}$. This is typically done by sampling from the prior distribution.

2. ***Prediction Step:***

- *Propagate Particles:* For each particle $x_t^{(i)}$, predict the next state of the system $x_{t+1}^{(i)}$ based on the system dynamics model f. This can be expressed as 8:

$$x_{t+1}^{(i)} = f(x_t^{(i)}, u_t) + \epsilon_t^{(i)} \tag{8}$$

where u_t represents any input applied at time t and $\epsilon_t^{(i)}$ is the process noise associated with the transition.

3. ***Update Step:***

- *Measurement Likelihood Calculation:* For each particle $x_{t+1}^{(i)}$, calculate the likelihood $p(z_{t+1}|x_{t+1}^{(i)})$ of the observed measurements z_{t+1} given the predicted state. This is computed using the measurement model h, which relates the state to the measurements:

$$\begin{aligned} p(z_{t+1}|x_{t+1}^{(i)}) &= \mathcal{N}(z_{t+1}; h(x_{t+1}^{(i)}), R_{t+1}) \\ &= \frac{1}{\sqrt{(2\pi)^k |R_{t+1}|}} \\ &\exp\left(-\frac{1}{2}(z_{t+1} - h(x_{t+1}^{(i)}))^T R_{t+1}^{-1}(z_{t+1} - h(x_{t+1}^{(i)}))\right) \end{aligned} \tag{9}$$

where $\mathcal{N}$ denotes the normal distribution, h is the measurement function, and R_{t+1} is the measurement noise covariance matrix.

- *Particle Weighting:* Compute the weight $w_{t+}^{(i)}$ for each particle based on its likelihood given the observed measurements:

$$w_{t+1}^{(i)} = \frac{p(z_{t+1}|x_{t+1}^{(i)})}{\sum_{j=1}^{N} p(z_{t+1}|x_{t+1}^{(j)})} \tag{10}$$

where N is the total number of particles.

4. ***Estimation Step:***

- *State Estimate Calculation:* Estimate the state of the system $x_{t+1}^{(i)}$ based on the weighted average of the particles:

$$\hat{x}_{t+1} = \sum_{i=1}^{N} w_{t+1}^{(i)} \cdot x_{t+1}^{(i)} \tag{11}$$

- *Uncertainty Estimation:* Estimate the uncertainty associated with the state estimate using the weighted covariance matrix:

$$\hat{P}_{t+1} = \sum_{i=1}^{N} w_{t+1}^{(i)} \cdot (x_{t+1}^{(i)} - \hat{x}_{t+1}) \cdot (x_{t+1}^{(i)} - \hat{x}_{t+1})^T \tag{12}$$

5. ***Iteration:***

- *Repeat Prediction, Update, and Estimation Steps:* Repeat the prediction, update, and estimation steps for each time step, continuously updating the state estimate as new measurements become available.

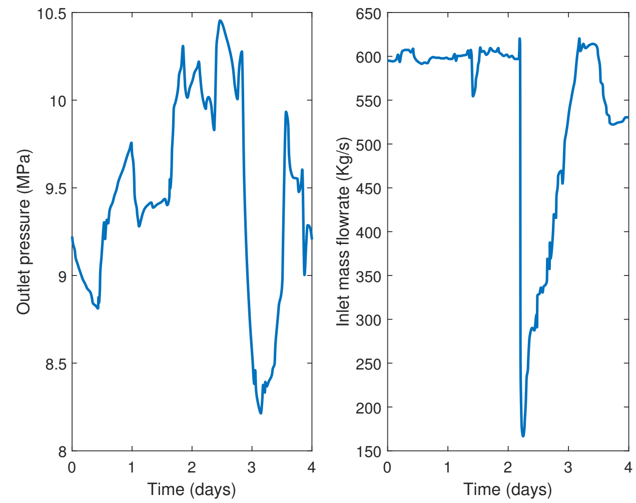

FIGURE 13: BOUNDARY CONDITIONS - OUTLET PRESSURE AT THE TOP AND INLET MASS FLOW RATE AT THE BOTTOM

4. RTTM-BASED LEAK DETECTION FOR NATURAL GAS PIPELINES USING THE ADVANCED MODEL

The widespread use of leak detection systems with short response time can significantly reduce the emissions in the event of a leak either small or a rupture.

Alberta Energy Regulator (AER) regulates over 440,000 km of pipeline in Alberta. This includes 251,000 km of natural gas and 24,000 km of sour natural gas pipelines with methane as the main component. According to AER, in 2022 the number of leak and rupture incidents in natural gas and sour natural gas pipelines are 90 resulted in an incident rate of 0.33 per 1000 km of pipeline.

Availability of reliable and cost-effective leak detection technologies encourage widespread adoption and let the regulators to issue new regulations and standards toward achieving net-zero.

The success of RTTM-based leak detection systems depends on the availability and quality of measurements along the pipeline and the knowledge of model parameters over time. The following sections explains the practicality and the limitations of the implementation of a RTTM-based leak detection using the advanced model presented in section 3, for natural gas pipelines under realistic conditions.

4.1 Instrumentation Availability

Having a well-instrumented pipeline or full-state measurements with sensors placed strategically at various locations, including pressure, flow rate, temperature, and density (a.k.a. the states of the system), provides a more complete picture of the pipeline's condition and enhances the system's ability to detect abnormalities indicative of leaks.

While having a well-instrumented pipeline with full measured states is ideal for RTTM-based leak detection systems, equipping pipelines with all necessary sensors for comprehensive monitoring poses several challenges, including high costs, logistical complexities, regulatory hurdles, and environmental considerations. Additionally, maintaining reliable power and communication infrastructure in remote areas and managing vast amounts

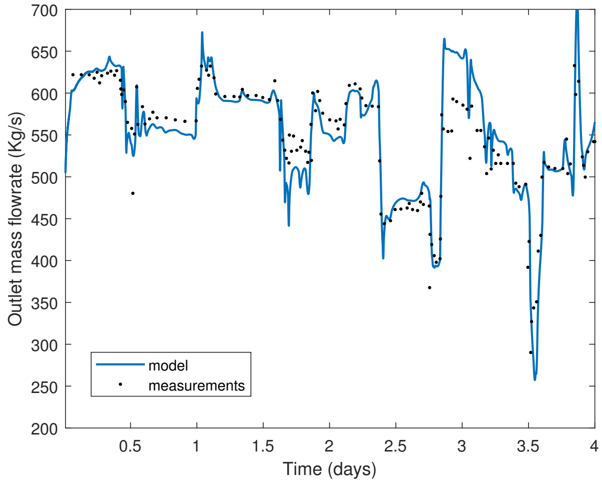

FIGURE 14: OUTET MASS FLOWRATE PREDICTED BY THE MODEL, BLACK DOTS AND SOLID BLUE LINE ARE MEASUREMENTS AND MODEL CALCULATIONS, RESPECTIVELY.

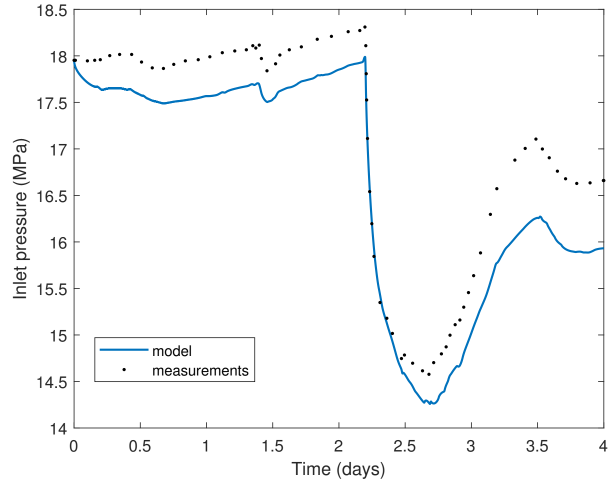

FIGURE 15: INLET PRESSURE PREDICTED BY THE MODEL, BLACK DOTS AND SOLID BLUE LINE ARE MEASUREMENTS AND MODEL CALCULATIONS, RESPECTIVELY.

of data generated by numerous sensors add further complexity.

It's not uncommon for natural gas pipelines to be inadequately instrumented, at which point leak detection systems can leverage advanced models employing estimators to compensate for the absence of certain measurements.

The minimal prerequisite for implementing RTTM-based leak detection using the proposed model is access to measurements of at least one variable (state) at the boundaries of the detection segment. Pressure readings are the most commonly available measurements. Leveraging pressure data at the boundaries enables the model to compute all other latent variables, including flow rates and pressures at internal nodes along the pipe length.

RTTM-based leak detection systems rely on comparing the observed states of the pipeline with the expected behavior predicted by the mathematical model. Hence, in addition to pressure readings at the boundaries, another known state is required, which could be obtained from intermediate pressure or temperature transmitters installed non-intrusively on any exposed sections of the pipeline.

4.2 Parameter Estimation

The parameters of the pipeline model, such as pipe roughness or fluid viscosity, may not be precisely known and could vary over time. Particle filters can handle model parameter uncertainty by treating these parameters as latent variables to be estimated alongside the state variables. This allows for robust estimation of pipeline conditions even in the presence of parameter uncertainties.

Below are some sources of uncertainty that state estimators adeptly handle, which could otherwise impede model predictions:

- Pipe specifications like roughness and elevation profile;
- Fluid properties such as viscosity, speed of sound, and gas composition;
- Environmental factors including soil thermal conductivity, ground depth, and ambient or soil temperatures.

Given that different parameters within the system may have distinct characteristics and uncertainties, opting for different probability density functions (PDFs) for various parameters could enhance the performance and efficiency of the filter, and better capture their individual behaviors and uncertainties.

5. RESULTS AND DISCUSSIONS

In this section the performance of the model presented in section 2 is validated using data from an industrial pipeline. The results are compared to the performance of the model after the integration of the particle filter as explained in section 3 to show the enhancements in the predictions after using an estimator.

The pipeline used for the validation of the model is a 650 km offshore natural gas transmission pipeline operated by Gasscos with inner diameter of 1.016 m. The measurement data for this pipeline has been taken from Helgaker Ph.D. thesis and is available in [13].

The pipeline is buried approximately 1.5 m under the ground for the first and last 25 km and it is at the bottom of the sea for the rest of its path. The molar composition of the gas as sampled is CH_4 (89.16%), C_2H_6 (7.35%), C_3H_8 (0.51%), $i-C_4H_{10}$ (0.03%), $n-C_4H_{10}$ (0.03%), $i-C_5H_{12}$ (0.001%),$n-C_5H_{12}$ (0.002%), N_2 (0.70%) and CO_2 (2.22%).

The inlet mass flow rate and the outlet pressure are set as boundary conditions for our model and presented in figure 13. The selected boundary conditions are typical transient operating condition for natural gas pipelines. Simulations were run and the available measurements for the inlet pressure and the outlet mass flow rate for four days period were used to verify the calculations of the model.

The calculated inlet pressure and outlet mass flow were shown in figures 14 and 15. The black dots are the measurements as presented in [13].

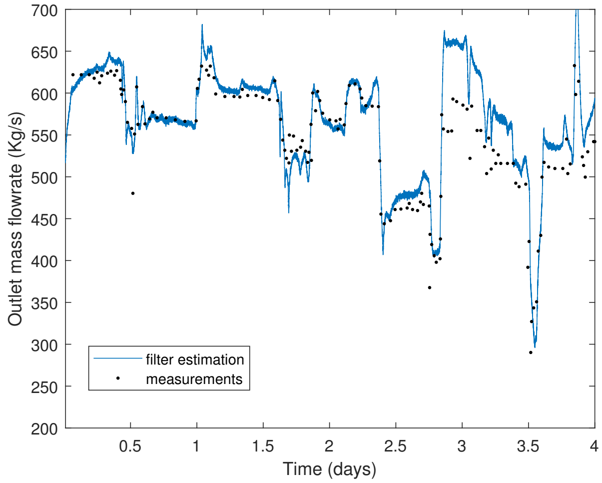

FIGURE 16: OUTLET MASS FLOW RATE ESTIMATED BY THE FILTER, BLACK DOTS AND SOLID BLUE LINE ARE MEASUREMENTS AND FILTER ESTIMATION, RESPECTIVELY.

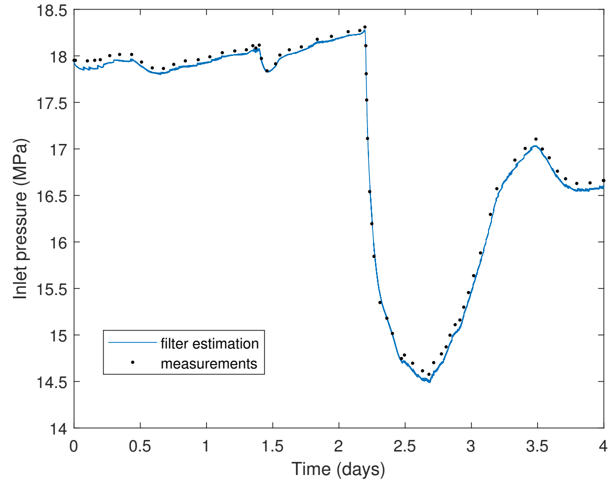

FIGURE 17: INLET PRESSURE ESTIMATED BY THE FILTER, BLACK DOTS AND SOLID BLUE LINE ARE MEASUREMENTS AND FILTER ESTIMATION, RESPECTIVELY.

The RTTM-based leak detection system can benefit from the advancement in state estimation techniques to compensate for the measurement noise and deal with uncertainties in the model parameters.

The designed particle filter has been customized and applied for the pipeline discussed in section 5. The filter estimations for the inlet pressure and outlet mass flow over time are shown in figures 16 and 17.

These plots illustrate how the particle filter tracks changes in the system states and provide insights into the accuracy and performance of the particle filter in capturing the system behavior.

The normalized root squared error (RSE) between the measurements and the model calculations is used to represent how well the results from the model follow the measured values. This provides a quantitative metrics to evaluate the accuracy of the predictions.

The normalized root squared error (RSE) between the measurements and the model calculations are presented in figure 18 for the inlet pressure at the top and the outlet mass flow rate at the bottom. Similarly, the normalized root squared error (RSE) between the measurements and the filter estimation are presented in figure 19.

As shown in figure 20, comparing to RSE from the model calculations, the error in the calculated inlet pressure using the particle filter has been significantly reduced and the residuals were minimized to help the leak detection system preventing false alarms. The error in the calculated outlet mass flow rates is almost the same.

The designed particle filter accounts for uncertainties in system parameters, data collection, and model calculations, allowing the model to adapt and make more accurate predictions or estimations in real-time scenarios.

The discrepancies observed in the measured and calculated values will be flagged as a possible leak event when it exceeds a certain threshold. The final decision to alarm can be made using a classification framework. The more accurate and robust predictions of the pipeline model through the particle filter enhance the ability to identify leaks of varying sizes in a short time-frame while minimizing the occurrence of false alarms.

6. CONCLUSION

The development and implementation of an RTTM-based leak detection system using a particle filter as the state estimator for pipelines transporting natural gas offer significant advantages in detecting leaks promptly and accurately. This timely detection facilitates proactive measures to mitigate the impact of leaks and prevent further escalation of incidents.

The particle filter is a Bayesian filtering technology based on Monte Carlo simulation. In essence, the integration of a particle filter into the model of the pipeline developed using the governing equations of the fluid dynamics, offers a hybrid model of the pipeline benefiting from both knowledge-based and data-driven approaches.

Through the utilization of particle filters, which are adept at handling nonlinear and non-Gaussian system dynamics, the proposed system can effectively estimate the state of the pipeline system and identify potential leak occurrences.

The particle filter framework allows the leak detection system to adapt to varying pipeline conditions and environmental factors. The proposed algorithm not only is successful in accurate prediction of the states but also capable of estimating the model parameters. The individual behaviors and uncertainties of different model parameters is better captured through utilizing customized probability density functions.

The results demonstrate the proposed model's efficacy in enhancing the accuracy and sensitivity of leak detection. The RTTM-based leak detection system employing particle filters represents a promising approach for reducing methane emissions and promoting sustainable pipeline management.

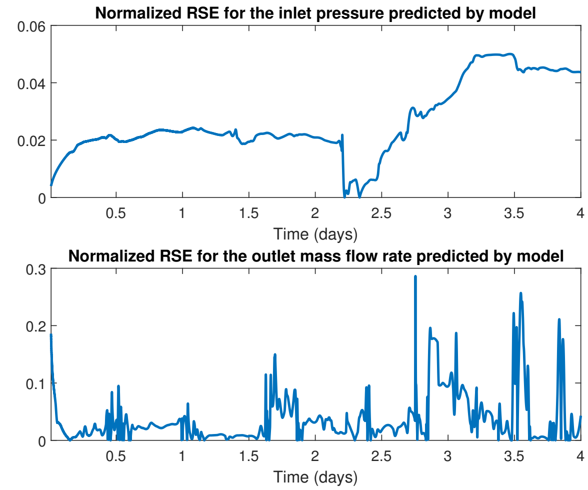

FIGURE 18: NORMALIZED RSE BETWEEN THE MODEL CALCULATIONS AND THE MEASUREMENTS, RSE FOR THE INLET PRESSURE AT THE TOP AND RSE FOR THE OUTLET MASS FLOW RATE AT THE BOTTOM.

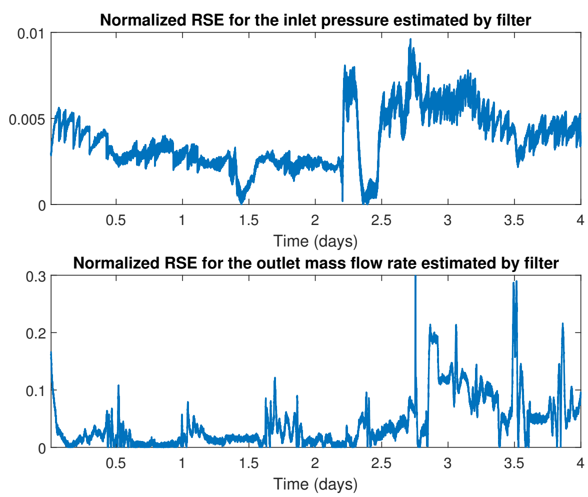

FIGURE 19: NORMALIZED RSE BETWEEN THE FILTER ESTIMATIONS AND THE MEASUREMENTS, RSE FOR THE INLET PRESSURE AT THE TOP AND RSE FOR THE OUTLET MASS FLOW RATE AT THE BOTTOM.

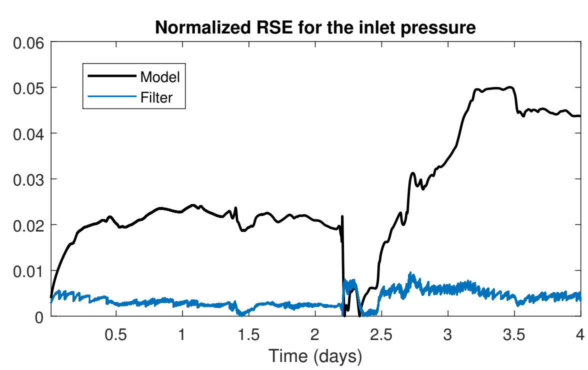

FIGURE 20: NORMALIZED RSE OF THE INLET PRESSURE AS PREDICTED BY MODEL (BLACK LINE) AND ESTIMATED BY THE FILTER (BLUE LINE).

REFERENCES

[1] Ghasvari-Jahromi, Hamed, Roxas, Michael and Mokamati, Satya. "Column Separation in a Shut-In Liquid Hydrocarbon Transmission Pipeline." Vol. Volume 3: Operations, Monitoring, and Maintenance; Materials and Joining: p. V003T04A027. 2018. DOI 10.1115/IPC2018-78743. URL https://asmedigitalcollection.asme.org/IPC/proceedings-pdf/IPC2018/51883/V003T04A027/2511889/v003t04a027-ipc2018-78743.pdf, URL https://doi.org/10.1115/IPC2018-78743.

[2] Ghasvari-Jahromi, Hamed, Ekram, Fatemeh, Roxas, Michael and Mokamati, Satya. "A Mathematical Model for the Spatial Prediction and Temporal Evolution of the Column Separation in a Flowing Hydrocarbon Transmission Pipeline.": pp. PSIG–1910. 2019. URL https://onepetro.org/PSIGAM/proceedings-pdf/PSIG19/All-PSIG19/PSIG-1910/1129977/psig-1910.pdf.

[3] Ghasvari-Jahromi, Hamed, Ekram, Fatemeh, Ali, Waqar, Roxas, Michael and Mokamati, Satya. "Performance of CPM Based Leak-Detection Algorithms in the Presence of Slack.": pp. PSIG–2103. 2021. URL https://onepetro.org/PSIGAM/proceedings-pdf/PSIG21/All-PSIG21/PSIG-2103/2447596/psig-2103.pdf.

[4] Zucrow, M. J. and Hoffman, J. D. *Gas dynamics, Vol. I*. John Wiley & Sons (1977).

[5] Ghasvari-Jahromi, Hamed, Ekram, Fatemeh, Deng, Chuntao, Knudson, Jim and Mokamati, Satya. "Real-Time Transient Modeling of CO2 pipelines and Phase Behavior During the Leak.": pp. PSIG–2430. 2024.

[6] Ghasvari-Jahromi, Hamed, Ekram, Fatemeh and Mokamati, Satya. "Supercritical Fluid Flow in Pipelines - A Dense Phase Case Study.": pp. PSIG–2324. 2023. URL https://onepetro.org/PSIGAM/proceedings-pdf/PSIG23/All-PSIG23/PSIG-2324/3115371/psig-2324.pdf.

[7] Setzmann, U. and Wagner, W. "A New Equation of State and Tables of Thermodynamic Properties for Methane Covering the Range from the Melting Line to 625 K at Pressures up to 1000 MPa." *Journal of Physical and Chemical Reference Data* Vol. 20 No. 6 (1991): pp. 1061–1155. DOI 10.1063/1.555898. URL https://pubs.aip.org/aip/jpr/article-pdf/20/6/1061/8183450/1061_1_online.pdf, URL https://doi.org/10.1063/1.555898.

[8] Chaczykowski, Maciej. "Transient flow in natural gas pipeline – The effect of pipeline thermal model." *Applied Mathematical Modelling* Vol. 34 No. 4 (2010): pp. 1051–1067. DOI https://doi.org/10.1016/j.apm.2009.07.017. URL https://www.sciencedirect.com/science/article/pii/S0307904X09002133.

[9] Herrán-González, A., De La Cruz, J.M., De Andrés-Toro, B. and Risco-Martín, J.L. "Modeling and simulation of a gas distribution pipeline network." *Applied Mathematical Modelling* Vol. 33 No. 3 (2009): pp. 1584–1600. DOI https://doi.org/10.1016/j.apm.2008.02.012. URL https://www.sciencedirect.com/science/article/pii/S0307904X08000607.

[10] Arulampalam, M.S., Maskell, S., Gordon, N. and Clapp, T. "A tutorial on particle filters for online nonlinear/non-

Gaussian Bayesian tracking." *IEEE Transactions on Signal Processing* Vol. 50 No. 2 (2002): pp. 174–188. DOI 10.1109/78.978374.

[11] Gopaluni, R. B. "A particle filter approach to identification of nonlinear processes under missing observations." *The Canadian Journal of Chemical Engineering* Vol. 86 No. 6 (2008): pp. 1081–1092. DOI https://doi.org/10.1002/cjce.20113. URL https://onlinelibrary.wiley.com/doi/pdf/10.1002/cjce.20113, URL https://onlinelibrary.wiley.com/doi/abs/10.1002/cjce.20113.

[12] Patwardhan, Sachin C., Narasimhan, Shankar, Jagadeesan, Prakash, Gopaluni, Bhushan and L. Shah, Sirish. "Nonlinear Bayesian state estimation: A review of recent developments." *Control Engineering Practice* Vol. 20 No. 10 (2012): pp. 933–953. DOI https://doi.org/10.1016/j.conengprac.2012.04.003. URL https://www.sciencedirect.com/science/article/pii/S0967066112000871. 4th Symposium on Advanced Control of Industrial Processes (ADCONIP).

[13] Helgaker, Jan Fredrik. "Modeling Transient Flow in Long Distance Offshore Natural Gas Pipelines." Phd thesis, Norwegian University of Science and Technology. 2013.